



Network-specific resting-state connectivity changes in the premotor-parietal axis in writer's cramp

Tobias Mantel^a, Tobias Meindl^a, Yong Li^a, Angela Jochim^a, Gina Gora-Stahlberg^a, Jona Kräenbring^{a,b}, Maria Berndt^c, Christian Dresel^{a,d}, Bernhard Haslinger^{a,*}

^a Department of Neurology, Klinikum rechts der Isar, Technische Universität München, Ismaningerstrasse 22, Munich, Germany

^b Department of Psychiatry, Isar-Amper-Klinikum München-Ost, Vockestrasse 72, Haar, Germany

^c Department of Neuroradiology, Klinikum rechts der Isar, Technische Universität München, Ismaningerstrasse 22, Munich, Germany

^d Department of Neurology, Johannes Gutenberg University, School of Medicine, Langenbeckstrasse 1, Mainz, Germany

ARTICLE INFO

Keywords:

Resting state
Functional connectivity
Dystonia
Premotor cortex
Cerebellum

ABSTRACT

Background: Writer's cramp is a task-specific dystonia impairing writing and sometimes other fine motor tasks. Neuroimaging studies using manifold designs have shown varying results regarding the nature of changes in the disease.

Objective: To clarify and extend the knowledge of underlying changes by investigating functional connectivity (FC) in intrinsic connectivity networks with putative sensorimotor function at rest in an increased number of study subjects.

Methods: Resting-state functional magnetic resonance imaging with independent component analysis was performed in 26/27 writer's cramp patients/healthy controls, and FC within and between resting state networks with putative sensorimotor function was compared. Additionally, voxel-based morphometry was carried out on the subjects' structural images.

Results: Patients displayed increased left- and reduced right-hemispheric primary sensorimotor FC in the premotor-parietal network. Mostly bilaterally altered dorsal/ventral premotor FC, as well as altered parietal FC were observed within multiple sensorimotor networks and showed differing network-dependent directionality. Beyond within-network FC changes and reduced right cerebellar grey matter volume in the structural analysis, the positive between-network FC of the cerebellar network and the basal ganglia network was reduced.

Conclusions: Abnormal resting-state FC in multiple networks with putative sensorimotor function may act as basis of preexisting observations made during task-related neuroimaging. Further, altered connectivity between the cerebellar and basal ganglia network underlines the important role of these structures in the disease.

1. Introduction

Writer's cramp (WC) is a task-specific focal hand dystonia (FHD) with a peak incidence between the 3rd and 5th decade causing abnormal and disabling postures through uncoordinated overflowing muscle activity solely during writing (simple WC) or also during fine motor tasks (dystonic WC) (Sheehy and Marsden, 1982). In the past, a number of neuroimaging studies have been conducted to further elucidate the yet not fully clear mechanisms of this disease, and both

functional and structural changes in the primary sensorimotor and the premotor/supplementary motor cortex, the cerebellum and basal ganglia have been described (Hallett, 2006; Neychev et al., 2011). During the last years, the concept of resting state functional connectivity (FC) networks has gained much attention. It refers to the observation that networks of brain regions temporally correlate by low frequency fluctuations of the blood oxygen level dependent (BOLD) signal in the absence of experimental tasks (Biswal et al., 1997; Cordes et al., 2001; Fox and Raichle, 2007). Interestingly, those spatial

Abbreviations: ADDS, arm dystonia disability scale; BGN, basal ganglia network; BOLD, blood oxygen level-dependent; CN, cerebellar network; CONTR, healthy controls; FC, functional connectivity; FHD, focal hand dystonia; FWHM, full width at half maximum; FoV, field of view; GM, grey matter; IC, independent component; ICA, independent component analysis; ICN, intrinsic connectivity network; IPS, intraparietal sulcus; M1, primary motor cortex; PAT, writer's cramp patients; PCA, principal component analysis; PPN, premotor parietal network; PMd/v, dorsal/ventral premotor cortex; S1, primary somatosensory cortex; ROI, region of interest; rsfMRI, resting state functional magnetic resonance imaging; S2, secondary somatosensory cortex; SMI, primary sensorimotor cortex; SMA, supplementary motor area; SMG, supramarginal gyrus; v/dSMN, ventral/dorsal sensorimotor network; SPC, superior parietal cortex; TIV, total intracranial volume; WC, writer's cramp; WCRS, writer's cramp rating scale

* Corresponding author at: Klinik und Poliklinik für Neurologie, Klinikum rechts der Isar, Technische Universität München, Ismaninger Strasse 22, D - 81675 München, Germany.

E-mail address: bernhard.haslinger@tum.de (B. Haslinger).

<http://dx.doi.org/10.1016/j.nicl.2017.10.001>

Received 11 July 2017; Received in revised form 12 September 2017; Accepted 2 October 2017

Available online 14 October 2017

2213-1582/ © 2017 The Authors. Published by Elsevier Inc. This is an open access article under the CC BY-NC-ND license (<http://creativecommons.org/licenses/by-nc-nd/4.0/>).

networks of temporally correlated brain areas have a distribution similar to what is observed in task activation studies, hinting at a common functionality. The correlation between the hubs in such networks has further been shown to increase in the presence of adequate tasks suggesting that task-related activity may constitute a superposition of spontaneous BOLD activity at rest (Fox and Raichle, 2007). In WC, task-based neuroimaging studies have promoted the identification of brain areas involved in this disease but, using various different experimental paradigms, yielded ambiguous results regarding the nature of changes. As an example, in FHD either reduced (Ibanez et al., 1999; Langbour et al., 2017; Nelson et al., 2009; Oga et al., 2002), increased (Lerner et al., 2004; Odergren et al., 1998) or opposed (Ceballos-Baumann et al., 1997) primary sensory (S1) and/or motor (M1) activity have been shown during sensory (Langbour et al., 2017; Nelson et al., 2009) or dystonic (Ceballos-Baumann et al., 1997; Lerner et al., 2004; Odergren et al., 1998) and asymptomatic (Ibanez et al., 1999; Oga et al., 2002) motor tasks. Studying the connectivity between brain regions in the absence of tasks might thus seem suitable to identify underlying changes in this disease. Still, earlier findings in resting state fMRI (rsfMRI) were not unequivocal. While one early rsfMRI study reported reduced left primary sensorimotor connectivity when investigating one sensorimotor network (Mohammadi et al., 2012), a seed-based approach reported increased connectivity between left S1 and M1 (Dresel et al., 2014) and had the constraint of a required prior spatial definition of regions of interest (ROIs). In this study, we aimed at further clarifying and possibly extending the knowledge of underlying changes in this disease by investigating cortical and subcortical intrinsic connectivity networks with attributed sensorimotor functionality applying an independent component based approach that avoids a possible bias induced by the choice of seed regions using an increased number of study subjects compared to previous trials. Additionally, a voxel-based morphometry analysis was performed to detect underlying grey matter changes as a possible cause of FC changes.

2. Methods

2.1. Participants

We investigated 26 WC patients (PAT; age 46.8 ± 13.7 years, m/f 15/11) and 27 healthy subjects (CONTR; age 49.3 ± 13.9 years, m/f 14/13) < 70 years of age with no neuro(psychiatric)/major internal disease, no neuroleptic or anticholinergic medication and a normal structural MRI, whose functional scans fulfilled the criteria of a composite (translation and rotation (Power et al., 2014)) head displacement of less than the voxel size in maximum and half the voxel size on average. No patient had received botulinum toxin therapy within the last three months prior to the study. The functional motor impairment of the hand was assessed with the arm dystonia disability scale (ADDS) for fine motor tasks, and specifically for writing using the writer's cramp rating scale (WCERS). The university ethics board approved the study. All participants gave their written informed consent according to the Declaration of Helsinki.

2.2. Data acquisition and preprocessing

For rsfMRI, 303 T2* echo-planar whole-brain functional MR images were acquired for each participant on a Philips Achieva 3.0 T scanner with an 8-channel head coil (TR/TE 2200/30 ms, field of view (FoV) $216 \times 216 \text{ mm}^2$, 36 slices, voxel size $3 \times 3 \times 3 \text{ mm}^3$, scan time 11 min). The participants were instructed to keep their eyes closed during the whole experiment. To minimize the risk of motion artifacts, the head was fixed with foam pads. After rsfMRI, a high-resolution 3D T1-weighted structural image was acquired for anatomical reference (TR/TE/TI 59/4/780 ms, FoV $240 \times 240 \text{ mm}^2$, 170 slices, voxel size $1 \times 1 \times 1 \text{ mm}^3$, scan time 6 min).

Preprocessing of functional data was performed in SPM12 (<http://www.fil.ion.ucl.ac.uk/spm>) and Matlab2013a (The MathWorks, Natick, Massachusetts), and involved realignment for head motion correction, slice timing correction, coregistration with the anatomical reference image and normalization to the Montreal Neurological Institute (MNI) space with resampling to $2 \times 2 \times 2 \text{ mm}^3$ voxels. The data were spatially smoothed with an isotropic Gaussian kernel of 8 mm full width at half maximum (FWHM). The first five scans of the rsfMRI run were discarded to ensure longitudinal magnetization equilibrium. The average framewise displacement (Power et al., 2014) (translation and rotation) was $0.10 \pm 0.03 \text{ mm}$ in PAT and $0.10 \pm 0.03 \text{ mm}$ in CONTR ($F_{1,51} = 0$, $p = 1.0$), the composite maximum head displacement $1.32 \pm 0.71 \text{ mm}$ in PAT and $1.15 \pm 0.53 \text{ mm}$ in CONTR ($F_{1,51} = 0.90$, $p = 0.35$) and the total intracranial volume (TIV) $1612.1 \pm 191.4 \text{ mm}^3$ in PAT and $1544.1 \pm 164.9 \text{ mm}^3$ in CONTR ($F_{1,51} = 1.96$, $p = 0.17$).

www.fil.ion.ucl.ac.uk/spm) and Matlab2013a (The MathWorks, Natick, Massachusetts), and involved realignment for head motion correction, slice timing correction, coregistration with the anatomical reference image and normalization to the Montreal Neurological Institute (MNI) space with resampling to $2 \times 2 \times 2 \text{ mm}^3$ voxels. The data were spatially smoothed with an isotropic Gaussian kernel of 8 mm full width at half maximum (FWHM). The first five scans of the rsfMRI run were discarded to ensure longitudinal magnetization equilibrium. The average framewise displacement (Power et al., 2014) (translation and rotation) was $0.10 \pm 0.03 \text{ mm}$ in PAT and $0.10 \pm 0.03 \text{ mm}$ in CONTR ($F_{1,51} = 0$, $p = 1.0$), the composite maximum head displacement $1.32 \pm 0.71 \text{ mm}$ in PAT and $1.15 \pm 0.53 \text{ mm}$ in CONTR ($F_{1,51} = 0.90$, $p = 0.35$) and the total intracranial volume (TIV) $1612.1 \pm 191.4 \text{ mm}^3$ in PAT and $1544.1 \pm 164.9 \text{ mm}^3$ in CONTR ($F_{1,51} = 1.96$, $p = 0.17$).

2.3. Group independent component analysis

Group spatial independent component analysis (ICA) on the rsfMRI data of each patient and healthy controls was performed as implemented in the GIFT v3.0 software (<http://mialab.mrn.org>). ICA estimates spatially maximally independent sources from the linearly mixed signals contained in a spatiotemporal fMRI dataset, providing spatial maps of temporally coherent brain regions (functional spatial networks) (Calhoun et al., 2001). This approach has been shown to effectively identify and remove various sources of motion and non-motion-related noise in fMRI data (Griffanti et al., 2014). Further, its suggested property of being sensitive to the detection of subtle changes (Koch et al., 2012) is desirable when investigating task-specific dystonia. The calculated spatially independent components (ICs) represent either meaningful (i.e. intrinsic connectivity networks (ICNs)) or spurious (e.g. noise) information.

In a first step, the number of components in the whole dataset was determined by a dimensionality estimation using the minimum description length algorithm resulting in an estimate of a maximum of 52 and a mean number of 33 ICs. Based on these estimates, a stepwise dimensionality reduction was performed in each group using principal component analysis (PCA) (Celone et al., 2006; Wu et al., 2011), retaining 52 components at the subject- and 33 components at the group-level. This was followed by IC separation using the InfoMax algorithm (Bell and Sejnowski, 1995). Reliability testing was performed using the ICASSO toolbox (Himberg et al., 2004): ICA was repeated 40 times, the components were clustered, and their quality quantified using the index I_q (range 0 to 1) which mirrors the difference between intra- and extra-cluster similarity. Back-reconstruction of subject-specific spatial maps was performed from the aggregate spatiotemporal data set using a method based on PCA compression and projection robust for low model orders (GICA I) (Calhoun et al., 2001). To identify components of likely functional relevance in WC for further analysis, the spatial IC maps were correlated with publicly available maps of ICNs identified in a meta-analysis of task fMRI studies performed by Laird and colleagues (Laird et al., 2011) using multiple regression. The non-noise IC with the best fit (highest coefficient of determination) was selected. ICs representing noise were identified by standardized visual inspection of their spatial (activation pattern and tissue overlap with grey matter (GM)) and temporal characteristics (e.g. presence of saw tooth and high frequency patterns or spikes) as previously described (Kelly et al., 2010). Those identified components with attributed sensorimotor function in the meta-analysis (Laird et al., 2011) were then selected for further analysis (see Fig. A.1): a basal ganglia-thalamus network (BGN, ~Laird's ICN3), a cerebellar network (CN, ~Laird's ICN14), a premotor-parietal network (PPN, ~Laird's ICN7), a dorsal sensorimotor network (dSMN, ~Laird's ICN8/9) and a ventral sensorimotor network (vSMN, ~Laird's ICN17). The primary visual network (VN, ~Laird's ICN12) was chosen as a control. All investigated components were highly stable ($I_q \geq 0.95$). All selected networks have been previously

described at rest (Allen et al., 2011; Beckmann et al., 2005; Smith et al., 2009). Other identified ICNs reported by Laird et al. not chosen for analysis are visualized in Fig. A.2.

2.3.1. Analysis of within-network FC

The corresponding single-subject spatial IC maps of each selected network were entered into within- and between-group *t*-tests in SPM12 to draw population-based inferences on the composition and FC of these RSNs. In addition to sex and age, the maximum composite total head displacement and the average framewise head displacement were included as regressors in the second-level model to control for possible residual head motion not accounted for by ICA. To correct for multiple voxel-wise comparisons, we applied a Bonferroni-corrected peak-level threshold of $p(\text{FDR}) < 0.0083$ ($p(\text{FDR}) < 0.05/6$ for six investigated ICNs) in addition to a cluster-level threshold of $p(\text{FWE}) < 0.05$. A combined binary mask from the within-group analyses was created to ensure that only highly connected regions of each network were analyzed.

2.3.2. Analysis of between-network FC

We calculated an estimate for the FC between the investigated ICNs by correlating the time courses of these ICNs in each subject. Processing of time courses involved the removal of linear, cubic and quadratic trends, despiking, filtering at a standard high-frequency cut-off of 15 Hz and regression of realignment parameters. The individual's Fisher's *z*-transformed Pearson correlation coefficients z_r were then compared between groups in an analysis of covariance including the covariates age and sex. The significance level was set at $p < 0.01$ ($p = 0.05/5$ for five comparisons/network).

2.4. Morphometric analysis

Voxel-based morphometry was performed using an optimized procedure as implemented in the CAT12 toolbox (<http://www.neuro.uni-jena.de/cat/>). Structural scans were skull-stripped, tissue segmented using the implemented adaptive maximum a posteriori approach (Rajapakse et al., 1997) and normalized to MNI space using DARTEL (diffeomorphic anatomical registration using exponentiated lie algebra). Jacobian modulation was performed on the resulting GM segments that were smoothed with an 8 mm FWHM isotropic Gaussian kernel. The significance level of the age, sex and TIV-adjusted between-group *t*-test was set at a peak-level threshold of $p < 0.001$ (uncorrected) with an additional cluster level-threshold at $p(\text{FWE}) < 0.05$. Trends are reported for a cluster-level threshold of $p(\text{FDR}) < 0.05$.

2.5. Post hoc correlation with clinical characteristics

Given a significant result in the above-described between-group analyses, separate post hoc multiple regression analyses with the clinical parameters disease duration, ADDS and WCRS were set up for the PAT group. Inclusion of nuisance regressors and correction for multiple comparisons was performed as in the respective between-group analyses.

3. Results

Statistical analysis revealed no significant between-group difference in age ($F_{1,51} = 0.41$, $p = 0.53$) or sex ($F_{1,51} = 0.18$, $p = 0.68$). The mean disease duration in PAT was 13.2 ± 10.8 years, the ADDS was rated $60.8 \pm 20.1\%$ and the WCRS 11.7 ± 5.4 points.

3.1. Analysis of within-network FC

The between-group analysis of the six ICNs revealed significant FC changes in all networks except the VN (Fig. 1, Tables 1, 2). The

networks and their spatial extent in each group are illustrated in Fig. A.1.

3.1.1. PPN

Increased FC in PAT was seen for the left lateral dorsal premotor cortex (PMd) and the left primary sensorimotor cortex (SM1, GM of the central sulcus). Reduced FC was observed for the right M1 and S1, supramarginal gyrus (SMG) and posterior superior parietal cortex (SPC) as well as for the medial intraparietal sulcus area (IPS) bilaterally. Further, we found reduced FC for the right caudal and rostral ventral premotor cortex (PMv) and bilateral inferior frontal sulcus area.

3.1.2. SMNs

Within the dSMN, PAT showed increased FC for the left ventromedial prefrontal cortex and reduced FC for the PMd and the supplementary motor area (SMA) bilaterally. Within the vSMN, there was increased FC in PAT for the temporo-occipital junction and there were no areas of significantly reduced FC.

3.1.3. CN

Increased FC in PAT was found for the posterior cerebellum and the caudal PMv bilaterally and reduced FC was observed for the left posterior SPC.

3.1.4. BGN

Increased FC in PAT was found for the PMd, PMv (with findings for the left PMd extending to the preSMA), posterior cerebellum and secondary somatosensory cortex (S2) bilaterally. Further, FC was increased for the left SM1, cingulate cortices and the right SMG and posterior SPC. Reduced FC in PAT was found for the caudate and thalamus bilaterally, as well as for the right pallidum and hippocampus.

3.2. Analysis of between-network FC

The analysis of inter-network FC revealed a significant reduction of positive FC between the CN and BGN ($F_{1,49} = 16.4$, $p = 0.0002$, $r = 0.51$) as well as the CN and VN ($F_{1,49} = 4.14$, $p = 0.003$, $r = 0.41$) in PAT (Figs. 2, A.3; Table 3).

3.3. Analysis of structural changes

Voxel-based morphometry revealed significantly reduced GM volume in PAT in the right posterior cerebellum ($x|y|z = 28|-64|-40$, $t = 4.31$, $k = 2478$) and a trend for reduced GM volume in the left posterior cerebellum ($x|y|z = -34|-74|-40$, $t = 4.42$, $k = 2159$; Fig. 1).

3.4. Correlation with clinical characteristics

Multiple regression did not reveal any significant correlation between disease duration, ADDS and WCRS with within- or between-network FC values in PAT. Multiple regression with voxel-wise GM values revealed a significant positive correlation between the score on the WCRS and GM volume in the left S2 ($x|y|z = -58|-22|32$, $t = 6.59$, $k = 1952$).

4. Discussion

WC patients displayed altered within-network FC at rest mainly in the dSMN, PPN, BGN and CN, involving various FC changes of primary sensorimotor, premotor and parietal cortices as well as of thalamus, basal ganglia and cerebellum. These encompassed in their entirety a web of regions previously identified as being active during the task of writing (Rijntjes et al., 1999). Parallel to this, for the cerebellum also structural changes of GM volume were shown.

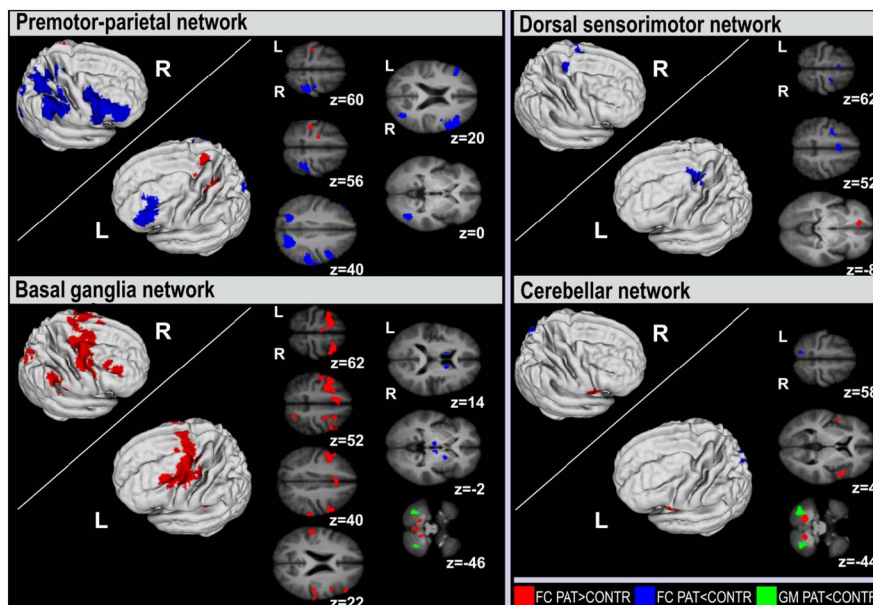


Fig. 1. Significant between-group differences of functional connectivity (FC) within the premotor-parietal, dorsal sensorimotor, basal ganglia and cerebellar network. Significant FC changes (p (FDR) < 0.0083, $p_{\text{cluster}}(\text{FWE})$ < 0.05) are overlaid onto the axial slices/3D reconstructions of the participants' averaged, skull-stripped T1 images. For the cerebellum, additionally structural changes including trends at $p_{\text{cluster}}(\text{FDR})$ < 0.05 are displayed. Slice positions in Montreal Neurological Institute space in mm are given relative to the anterior commissure (z above/below [+]/[-]). CONTR, healthy controls; PAT, writer's cramp patients; L/R, left/right hemisphere.

4.1. Primary sensorimotor cortices

We observed abnormal FC of the primary sensorimotor cortex hand area(s) in patients within the PPN, showing increased left-hemispheric SM1 FC and a reduced right-hemispheric S1 and M1 FC. Additionally, there was increased left-hemispheric SM1 FC within the BGN. A previous ICA-based study investigating 16 WC patients described reduced left SM1 FC in the sensorimotor network (Mohammadi et al., 2012) in which we did not observe altered SM1 FC. The increased FC in the hemisphere contralateral to the dystonic hand is in line with the observation of increased S1-to-M1 FC in a recent seed-based rsfMRI study (Dresel et al., 2014). During task-related fMRI primary sensorimotor overactivity was seen when a dystonic task was involved (Preibisch et al., 2001), while the opposite was mainly observed in context of nondystonic interventions (simple motor tasks/sensory stimulation) (Langbour et al., 2017; Nelson et al., 2009; Oga et al., 2002). For S1, also altered functional topography of dystonic/non-dystonic body parts in task-induced FHDs has been shown (Meunier et al., 2001; Nelson et al., 2009). In analogy to the findings of task activation studies in FHD, our finding of increased FC of the dystonic hands' left-hemispheric SM1 representation may represent a correlate of defective intracortical inhibition and/or malfunctional plasticity that have been shown for FHD both in the left S1 and M1 (Quartarone and Hallett, 2013). Beyond intracortical changes, there is evidence for abnormal interhemispheric inhibition in FHD (Nelson et al., 2010; Niehaus et al., 2001). We observed increased left- and reduced right-hemispheric FC within the PPN. In healthy subjects unilateral motor tasks/tactile stimulation of the hand during fMRI lead to a contralateral increase and an ipsilateral reduction in M1/S1 BOLD activity which is assumed to mirror interhemispheric interactions (Eickhoff et al., 2008; Hamzei et al., 2002). Neurophysiologic studies in FHD reported reduced interhemispheric inhibition (right to left) of the right dystonic hand's M1 representation at rest (Nelson et al., 2010), and increased interhemispheric inhibition (left to right) of the unaffected left hand's M1 representation during muscle contraction (Niehaus et al., 2001). Congruently, transcranial dual current stimulation during bimanual mirrored finger movements reduced dystonic symptoms in musician's dystonia of the right hand when reducing the excitability of the left and increasing the excitability of the right M1 (Furuya et al., 2014). Thus, our observations within the PPN may provide some correlate for an abnormal interhemispheric interaction.

4.2. Premotor and parietal dysconnectivity

We observed multiple FC changes of the premotor cortex (PMC) affecting mostly the SMA, PMd and PMv. First, reduced bilateral SMA FC was seen within the dSMN, a network that has been linked to tasks involving hand action (Laird et al., 2011). Consistently, activity of the SMA was found reduced in most (Ceballos-Baumann et al., 1997; Ibanez et al., 1999; Lerner et al., 2004; Oga et al., 2002) task-based WC fMRI studies and contingent negative variation (attributed to a thalamo-SMA circuit (Nagai et al., 2004)) is reduced in WC (Hamano et al., 1999).

Second, we observed FC changes of the PMd within various ICNs. FC increases were seen in patients within the BGN bilaterally and the PPN (a mainly cortical network functionally associated with visuomotor task performance (Laird et al., 2011)) in the left hemisphere, and a FC reduction in patients was observed bilaterally within the dSMN. The PMd is found active during visuomotor tasks of the upper extremity and assumed to integrate multisensory information to compose task-adequate motor programs; it may further be involved in their subsequent execution (Hoshi and Tanji, 2007). Transcranial magnetic stimulation over the left-hemispheric PMd in healthy subjects interferes with hand motor sequences during visuomotor tasks (Schluter et al., 1998), the latter being dysfunctional in task-specific FHD (Granert et al., 2011). Motor task-related fMRI studies in WC reported both increased (Ceballos-Baumann et al., 1997; Lerner et al., 2004; Odegren et al., 1998) and reduced (Ibanez et al., 1999; Langbour et al., 2017) dorsal premotor activity.

Third, patients showed altered FC predominantly for caudal PMv domains (Brodmann's area 6). Increased FC was observed bilaterally within the CN and BGN and reduced FC was found within the PPN. In the latter, findings had right-hemispheric emphasis and also encompassed rostral PMv domains. Though the rostral PMv has classically been linked to speech, it has reliably been demonstrated to be also active during hand action (Rizzolatti et al., 2002). PMv areas are involved in the matching of multisensory input (esp. visuospatial information) to ongoing motor performance, thus enabling grip precision (Hoshi and Tanji, 2007; Rizzolatti et al., 2002) which has been shown to be impaired in FHD (Nowak et al., 2005).

Integrated multisensory information reaches the PMCs via the posterior parietal cortex (PPC). Its upper domain, the SPC, is suggested to provide integrated somatosensory and visual inputs to the PMd (Scheperjans et al., 2008). In the present study FC in patients was increased for the right SPC within the BGN, and reduced within the CN in

Table 1
Differences of functional connectivity in sensorimotor networks with predominantly cortical extent.

Area	x	y	z	t value	Cluster volume
Premotor-parietal network					
PAT > CONTR					
L lateral dorsal premotor, caudal (BA6)	-18	-12	56	5.17	48
L primary sensorimotor (BA3/4)	-34	-26	56	5.37	121
PAT < CONTR					
R supramarginal gyrus (BA40)	50	-34	36	6.34	1551
R superior parietal, caudal (BA7)	30	-42	50	5.50	
R primary somatosensory (BA2/5)	38	-36	62	5.21	
R primary motor (BA4)	34	-22	64	4.78	
R intraparietal sulcus (BA7)	22	-64	34	7.14	1102
L intraparietal sulcus (BA7)	-20	-62	38	5.65	339
R inferior frontal sulcus (BA46)	52	36	8	7.26	1581
R ventral premotor, rostral (BA9/46)	56	24	24	7.14	
R ventral premotor, rostral (BA44/45)	56	14	18	6.87	
R ventral premotor, caudal (BA6)	44	2	34	5.56	
R inferior frontal sulcus (BA46)	50	30	16	4.90	
L inferior frontal sulcus (BA46)	-46	-30	16	4.45	409
R temporo-occipital junction (BA19/37)	42	-64	-2	5.82	410
Dorsal sensorimotor network					
PAT > CONTR					
L ventral medial prefrontal (BA11/32)	-12	44	-8	6.33	45
PAT < CONTR					
R supplementary motor (BA6)	2	8	54	6.29	164
L supplementary motor (BA6)	-2	4	58	5.36	
R lateral dorsal premotor, caudal (BA6)	24	-10	60	5.55	23
L lateral dorsal premotor, caudal (BA6)	-28	-6	52	5.15	76
Ventral sensorimotor network					
PAT > CONTR					
R temporo-occipital junction (BA19/37)	50	-74	2	5.92	91
PAT < CONTR					
-	-	-	-	-	-

Coordinates (in mm) in the Montreal Neurological Institute space. All FC differences are significant at $p < 0.0083$ (FDR) and $p < 0.05$ cluster at the cluster-level. PAT, writer's cramp patients; CONTR, healthy controls; R, right; L, left; ant., anterior (rostral), post., posterior (caudal). The term sensorimotor cortex describes maxima located in the central sulcus of the anatomical mean image that were not unequivocally assignable to the primary sensory or motor area.

the left, and the PPN in the right hemisphere. Its lower domain, the inferior parietal cortex, is linked to the PMv. Here, we found the FC for the right SMG to be reduced within the dSMN and increased in the BGN. Further, the FC of GM encompassing the medial IPS area was reduced bilaterally within the PPN. The IPS area has been suggested to serve as an integration interface between perceptive systems and the PMv, with its medial parts assumed to play an important role in visuomotor coordination of hand motion (Grefkes and Fink, 2005; Hoshi and Tanji, 2007). Together with above-described premotor changes, these findings in the PPN fit well with the observation of reduced PMv-PPC connectivity during writing (Gallea et al., 2016) and in a seed-based approach at rest (Delnooz et al., 2012). The significance of the greater right-hemispheric extent of findings in the parietal cortex and the PMv remains unclear. One may hypothesize if they could be the result of a right-hemisphere emphasis of the activity of the frontoparietal mirror neuron system. Recently fMRI provided evidence for an emphasized activation of this system in the hemisphere ipsilateral to the visual hemifield in which a certain object-oriented action is performed (Aziz-Zadeh et al., 2006). Thus, our observation may reflect the main

Table 2
Differences of functional connectivity changes in sensorimotor networks with predominantly subcortical/cerebellar extent.

Area	x	y	z	t value	Cluster volume
Cerebellar network					
PAT > CONTR					
L cerebellum, post. (VIII)	-14	-60	-42	7.66	124
R cerebellum, post. (VIII)	14	-62	-42	6.45	78
R ventral premotor, caudal (BA44)	54	8	6	5.90	118
L ventral premotor, caudal (BA44)	-46	2	2	4.87	39
PAT < CONTR					
L superior parietal, caudal (BA7)	-10	-60	58	4.83	39
Basal ganglia network					
PAT > CONTR					
L cerebellum, post (VIII)	-14	-67	-46	6.09	375
R cerebellum, post (IX)	12	-50	-44	4.75	93
L cingulum, posterior (BA32)	-6	-14	46	5.26	399
R cingulum, anterior (BA32)	8	20	38	4.27	
L cingulum, anterior (BA32)	-2	16	42	4.16	
L lateral dorsal premotor, rostral (BA44)	-46	6	4	7.62	1778
L pre-supplementary motor (BA6)	-22	10	52	6.86	
L lateral dorsal premotor/frontal eye field (BA6)	-34	2	60	6.73	
L inferior frontal junction (BA9)	-48	16	34	5.81	
L primary sensorimotor (BA3/4)	-46	-14	50	5.04	
R ventral premotor, caudal (BA6)	54	6	44	5.47	1006
R lateral dorsal premotor, rostral (BA6)	26	10	62	6.83	
R lateral dorsal premotor, caudal (BA6)	28	-10	54	4.55	
L secondary somatosensory (BA40)	-58	-28	16	7.08	113
R supramarginal gyrus (BA40)	64	-28	40	5.98	102
R secondary somatosensory (BA40)	48	-26	22	4.50	81
R superior parietal, caudal (BA7)	24	-60	54	4.39	77
PAT < CONTR					
L thalamus, ventral	-6	-16	-6	5.67	59
R thalamus, ventral	8	-14	-6	6.19	70
L caudate, corpus	-12	14	6	6.92	109
R caudate, corpus	14	6	14	6.49	192
R pallidum	18	4	0	5.47	
R hippocampus	22	2	-16	6.45	122

Coordinates (in mm) in the Montreal Neurological Institute space. All FC differences are significant at $p < 0.0083$ (FDR) and $p < 0.05$ cluster at the cluster-level. PAT, writer's cramp patients; CONTR, healthy controls; R, right; L, left; ant., anterior (rostral), post., posterior (caudal). The term sensorimotor cortex describes maxima located in the central sulcus of the anatomical mean image that were not unequivocally assignable to the primary sensory or motor area.

occurrence of writing in right-handers in the right visual hemifield.

An abnormal processing of (multi)sensory input is another key pathophysiologic concept in dystonia. It is suggested to lead to impaired sensorimotor integration in the disease, resulting in dystonic posture through loss of coordinated muscle activity (Quartarone and Hallett, 2013). Dysfunctional sensory processing in dystonia becomes evident in altered tactile spatiotemporal detection thresholds, vibration sense and mental rotation (Stamelou et al., 2012), with especially the latter pointing to an involvement of higher parietal areas. Abnormal integration at the premotor-parietal level has been discussed as foundation of task-specificity in WC (Hallett, 2006). Neuroimaging studies reporting parietal activity changes mostly reported reduced activity in the disease (Ceballos-Baumann et al., 1997; Langbour et al., 2017; Moore et al., 2012). Sensory tricks can improve dystonic symptoms (Stamelou et al., 2012), and amelioration of reduced PPC activity has been shown during sensory tricks in cervical dystonia (Naumann et al., 2000).

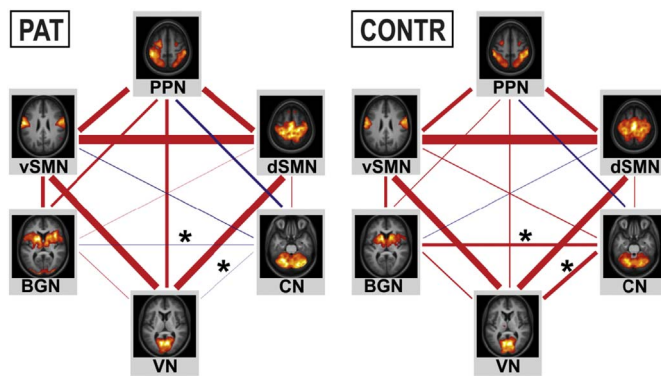


Fig. 2. Visualization of between-network functional connectivity in writer's cramp patients and healthy controls. The line thickness is proportional to the strength of positive (red) or negative (blue) time course correlation. Asterisks mark significant ($p < 0.01$) between-group differences. CONTR, healthy controls; PAT, writer's cramp patients; PPN, premotor parietal network; dSMN, dorsal sensorimotor network; vSMN ventral sensorimotor network; CN, cerebellar network; BGN, basal ganglia network; VN, medial visual network. (For interpretation of the references to color in this figure legend, the reader is referred to the web version of this article.)

Table 3
Matrix of between-network functional connectivity.

ICN	PMN	dSMN	vSMN	BGN	CN	VN
PAT						
PMN	1	0.3591	0.3355	0.1496	-0.1503	0.1984
dSMN	0.3591	1	0.5438	0.0170	0.0453	0.4085
vSMN	0.3355	0.5438	1	0.2231	-0.0445	0.4127
BGN	0.1496	0.0170	0.2231	1	-0.0207	0.0272
CN	-0.1503	0.0453	-0.0445	-0.0207	1	-0.0105
VN	0.1984	0.4085	0.4127	0.0272	-0.0105	1
CONTR						
PMN	1	0.2813	0.2478	0.0496	-0.1051	0.0736
dSMN	0.2813	1	0.5739	-0.0302	0.0457	0.3852
vSMN	0.2478	0.5739	1	0.1713	0.0586	0.3920
BGN	0.0496	-0.0302	0.1713	1	0.1923	0.0801
CN	-0.1051	0.0457	0.0586	0.1923	1	0.2416
VN	0.0736	0.3852	0.3920	0.0801	0.2416	1

Pairwise correlations between the ICN's time courses were Fisher z-transformed, averaged across the subjects in each group and subsequently inverse z-transformed for display. Significant results ($p < 0.01$) are highlighted in bold.

4.3. Cerebellar and basal ganglia circuits

Growing evidence suggests a role not only of the basal ganglia, but also the cerebellum in dystonia (Neychev et al., 2011; Shakkottai et al., 2017). Lesions of both basal ganglia and (rarely) cerebellum can cause dystonia (LeDoux and Brady, 2003), and both structures have been found to modulate cortical sensorimotor excitability (Restuccia et al., 2001; Tamburin et al., 2004). While some have argued for a mostly compensatory role of a dysfunctional basal ganglia-cerebellar interaction, alternative suggestions of primary defect have been made (Neychev et al., 2011; Shakkottai et al., 2017).

In the BGN, FC changes at the cortical level were focused on an increase in the dorsal > ventral PMC and in executive anterior cingulate areas. Additionally, FC changes in the left SM1 and bilateral S2, a relay for sensorimotor integration, were seen. In the latter, a lower left-hemispheric GM volume was associated with lower scores (= less impairment) on the WCRS. The basal ganglia enable learning of skilled movements and precise selection of movements in motor sequences (Mink, 1996). Dysfunctional surround inhibition resulting in impaired gating of (motor-related) sensory and motor information in the basal ganglia in FHD has been suggested as the cause of dystonic muscle co-activation (Quartarone and Hallett, 2013). Increased FC of the PMCs and bilaterally reduced FC of the corpus of the caudate nucleus and

thalamus within the BGN might hence reflect reduced inhibitory basal ganglia influence. Earlier neuroimaging has shown both reduced and increased activity in the thalamus (Ceballos-Baumann et al., 1997; Oergren et al., 1998) and basal ganglia (Gallea et al., 2016; Peller et al., 2006) as well as altered motor putaminal functional topography (Delmaire et al., 2005) in FHD. Seed-based studies observed reduced connectivity of putaminal or pallidal ROIs to primary sensory (motor) cortices during a non-dystonic finger tapping, dystonic writing (Gallea et al., 2016; Moore et al., 2012) and at rest (Dresel et al., 2014). FC changes within the CN at the cortical level were focused on the left SPC and the bilateral PMv, both areas with an emphasis on multisensory integration. The cerebellum processes considerable sensory input. Within the concept of internal forward models, it is thought to quickly provide information about the expected sensory consequences of motor commands enabling appropriate selection and rapid adaption of motor programs (Baumann et al., 2015). Altered FC of the PMv and SPC within the CN, but also between the CN and VN (similarly observed previously in embouchure dystonia (Haslinger et al., 2016)) hints at a disruption of cerebellar sensory integration in dystonia. Dresel et al. recently observed increased anticorrelation of cerebellar ROIs to multiple cortical areas (Dresel et al., 2014). The concept of disturbed cerebello-cortical interaction in WC is supported by Hubsch and colleagues, who reported a loss of cerebellar capacity to modulate motor cortical plasticity in the presence of sensory input (Hubsch et al., 2013). At the cerebellar level, we found increased FC of the posterior sensorimotor cerebellum in the CN and BGN. Increased cerebellar activity has been frequently reported during dystonic writing (Ceballos-Baumann et al., 1997; Oergren et al., 1998). Studies in patients with structural cerebellar disease suggest that cerebellar output modulates primary sensory/motor cortical excitability (Restuccia et al., 2001; Tamburin et al., 2004). Structurally, this study confirmed previous observations by Delmaire and colleagues of reduced cerebellar GM density (Delmaire et al., 2007). The present study did not observe a direct spatial overlap of FC and structural changes, whose potential relationship thus remains unclear.

In a mouse model, increased cerebellar and reduced basal ganglia function led to dystonia (Neychev et al., 2008), though results from mouse studies have to be interpreted carefully. In this respect, the present study further made the interesting finding of a loss of between-network CN-to-BGN FC at rest, while the between-network FC of the CN to the PPN and v/dSMN was unchanged. Recent task-based studies suggested a disruption of striatal and cerebellar interaction during motor learning in FHD (Shakkottai et al., 2017), and Neumann et al. observed inverse correlation of pallido-cerebellar coupling and dystonic symptom severity in primary dystonia when investigating local field potentials that have been shown to correlate with the fMRI BOLD response (Magri et al., 2012; Neumann et al., 2015). All this supports the notion of a dysfunctional cerebellar-basal ganglia interaction in dystonia.

Significant correlations of FC values and measures of disease duration and severity were not observed in our sample. In the past, some functional neuroimaging studies have observed such correlations (Dresel et al., 2014; Peller et al., 2006) while others did not (Haslinger et al., 2016; Langbour et al., 2017). Besides methodological differences between studies, the reason for these mixed findings remains yet unclear.

5. Conclusion

The present study observed multiple and network-specific FC changes in primary and especially higher-order sensory and motor networks at rest. The involvement of multiple sensorimotor networks primarily or secondarily affected by the disease may act as basis of the preexisting observations in task-related fMRI studies. Further, we found supportive evidence for a disrupted interaction between the cerebellar and basal ganglia network at rest. Our findings underpin the concept of

dystonia as a network disorder centered around possible basal ganglia and/or cerebellar dysfunction. At the end, functional imaging as applied in this study does not ultimately allow discriminating if the results are an endophenotype or at least in part secondary or compensatory for dystonia. Further study is needed to better understand the underlying structural correlates of the observed neuronal network changes in this disease.

Acknowledgements

We cordially thank all subjects who took part in this study.

Ethics approval

The study has been approved by the local ethics review board and written informed consent was obtained from all subjects.

Funding

This work was supported by the Deutsche Forschungsgemeinschaft (DFG HA3370/5-1), Bonn, Germany.

Disclosures concerning the present manuscript

T.M. has received research support from the KKF (Klinikum rechts der Isar, Muenchen) (E03-15). C.D. has received research support from the German Research Foundation (DFG) (DFG HA3370/3-1) and the KKF (Klinikum rechts der Isar, Muenchen). B.H. receives research support from the German Research Foundation (DFG) (DFG HA3370/5-1) and Ipsen. The other authors report no disclosures.

Full financial disclosures for the previous 12 months

T. Mantel has received travel grants by Merz Pharmaceuticals GmbH, AbbVie Deutschland GmbH and Bayer Vital GmbH. T. Meindl has received travel grants from Merz Pharmaceuticals GmbH, Ipsen Pharma GmbH and Pharm-Allergan GmbH. B.H. receives research support from Ipsen Pharma GmbH and DFG, has received speaker honoraria from Pharm-Allergan GmbH, Bayer Health Care Pharmaceuticals and Ipsen Pharma GmbH and has received travel grants from Ipsen Pharma GmbH and Merz Pharmaceuticals GmbH. He has received royalties for book chapters from Cambridge University Press and Springer Medizin. The other authors report no disclosures.

Appendix A. Supplementary data

Supplementary data to this article can be found online at <https://doi.org/10.1016/j.nicl.2017.10.001>.

References

Allen, E.A., Erhardt, E.B., Damaraju, E., Gruner, W., Segall, J.M., Silva, R.F., Havlicek, M., Rachakonda, S., Fries, J., Kalyanam, R., Michael, A.M., Caprihan, A., Turner, J.A., Eichele, T., Adelsheim, S., Bryan, A.D., Bustillo, J., Clark, V.P., Feldstein Ewing, S.W., Filbey, F., Ford, C.C., Hutchison, K., Jung, R.E., Kiehl, K.A., Kodituwakku, P., Komesu, Y.M., Mayer, A.R., Pearson, G.D., Phillips, J.P., Sadek, J.R., Stevens, M., Teuscher, U., Thoma, R.J., Calhoun, V.D., 2011. A baseline for the multivariate comparison of resting-state networks. *Front. Syst. Neurosci.* 5, 2.

Aziz-Zadeh, L., Koski, L., Zaidel, E., Mazziotta, J., Iacoboni, M., 2006. Lateralization of the human mirror neuron system. *J. Neurosci.* 26, 2964–2970.

Baumann, O., Borra, R.J., Bower, J.M., Cullen, K.E., Habas, C., Ivry, R.B., Leggio, M., Mattingley, J.B., Molinari, M., Moulton, E.A., Paulin, M.G., Pavlova, M.A., Schmammann, J.D., Sokolov, A.A., 2015. Consensus paper: the role of the cerebellum in perceptual processes. *Cerebellum* 14, 197–220.

Beckmann, C.F., DeLuca, M., Devlin, J.T., Smith, S.M., 2005. Investigations into resting-state connectivity using independent component analysis. *Philos. Trans. R. Soc. Lond. Ser. B Biol. Sci.* 360, 1001–1013.

Bell, A.J., Sejnowski, T.J., 1995. An information-maximization approach to blind separation and blind deconvolution. *Neural Comput.* 7, 1129–1159.

Biswal, B.B., Van Kylen, J., Hyde, J.S., 1997. Simultaneous assessment of flow and BOLD

signals in resting-state functional connectivity maps. *NMR Biomed.* 10, 165–170.

Calhoun, V.D., Adali, T., Pearson, G.D., Pekar, J.J., 2001. A method for making group inferences from functional MRI data using independent component analysis. *Hum. Brain Mapp.* 14, 140–151.

Ceballos-Baumann, A.O., Sheehan, G., Passingham, R.E., Marsden, C.D., Brooks, D.J., 1997. Botulinum toxin does not reverse the cortical dysfunction associated with writer's cramp. A PET study. *Brain* 120 (Pt 4), 571–582.

Celone, K.A., Calhoun, V.D., Dickerson, B.C., Atri, A., Chua, E.F., Miller, S.L., DePeau, K., Rentz, D.M., Selkoe, D.J., Blacker, D., Albert, M.S., Sperling, R.A., 2006. Alterations in memory networks in mild cognitive impairment and Alzheimer's disease: an independent component analysis. *J. Neurosci.* 26, 10222–10231.

Cordes, D., Haughton, V.M., Arfanakis, K., Carew, J.D., Turski, P.A., Moritz, C.H., Quigley, M.A., Meyerand, M.E., 2001. Frequencies contributing to functional connectivity in the cerebral cortex in "resting-state" data. *AJNR Am. J. Neuroradiol.* 22, 1326–1333.

Delmaire, C., Krainik, A., Tezenas du Montcel, S., Gerardin, E., Meunier, S., Mangin, J.F., Sangla, S., Garnero, L., Vidailhet, M., Lehericy, S., 2005. Disorganized somatotopy in the putamen of patients with focal hand dystonia. *Neurology* 64, 1391–1396.

Delmaire, C., Vidailhet, M., Elbaz, A., Bourdain, F., Bleton, J.P., Sangla, S., Meunier, S., Terrier, A., Lehericy, S., 2007. Structural abnormalities in the cerebellum and sensorimotor circuit in writer's cramp. *Neurology* 69, 376–380.

Delnooz, C.C., Helmich, R.C., Toni, I., van de Warrenburg, B.P., 2012. Reduced parietal connectivity with a premotor writing area in writer's cramp. *Mov. Disord.* 27, 1425–1431.

Dresel, C., Li, Y., Wilzeck, V., Castrop, F., Zimmer, C., Haslinger, B., 2014. Multiple changes of functional connectivity between sensorimotor areas in focal hand dystonia. *J. Neurol. Neurosurg. Psychiatry* 85, 1245–1252.

Eickhoff, S.B., Grefkes, C., Fink, G.R., Zilles, K., 2008. Functional lateralization of face, hand, and trunk representation in anatomically defined human somatosensory areas. *Cereb. Cortex* 18, 2820–2830.

Fox, M.D., Raichle, M.E., 2007. Spontaneous fluctuations in brain activity observed with functional magnetic resonance imaging. *Nat. Rev. Neurosci.* 8, 700–711.

Furuya, S., Nitsche, M.A., Paulus, W., Altenmuller, E., 2014. Surmounting retraining limits in musicians' dystonia by transcranial stimulation. *Ann. Neurol.* 75, 700–707.

Gallea, C., Horowitz, S.G., Ali Najee-Ullah, M., Hallett, M., 2016. Impairment of a parieto-premotor network specialized for handwriting in writer's cramp. *Hum. Brain Mapp.* 37, 4363–4375.

Granert, O., Peller, M., Jabusch, H.C., Altenmuller, E., Siebner, H.R., 2011. Sensorimotor skills and focal dystonia are linked to putaminal grey-matter volume in pianists. *J. Neurol. Neurosurg. Psychiatry* 82, 1225–1231.

Grefkes, C., Fink, G.R., 2005. The functional organization of the intraparietal sulcus in humans and monkeys. *J. Anat.* 207, 3–17.

Griffanti, L., Salimi-Khorshidi, G., Beckmann, C.F., Auerbach, E.J., Douaud, G., Sexton, C.E., Zsoldos, E., Ebmeier, K.P., Filippini, N., Mackay, C.E., Moeller, S., Xu, J., Yacoub, E., Baselli, G., Ugurbil, K., Miller, K.L., Smith, S.M., 2014. ICA-based artefact removal and accelerated fMRI acquisition for improved resting state network imaging. *NeuroImage* 95, 232–247.

Hallett, M., 2006. Pathophysiology of writer's cramp. *Hum. Mov. Sci.* 25, 454–463.

Hamano, T., Kaji, R., Katayama, M., Kubori, T., Ikeda, A., Shibasaki, H., Kimura, J., 1999. Abnormal contingent negative variation in writer's cramp. *Clin. Neurophysiol.* 110, 508–515.

Hamzei, F., Dettmers, C., Rzanny, R., Liepert, J., Buchel, C., Weiller, C., 2002. Reduction of excitability ("inhibition") in the ipsilateral primary motor cortex is mirrored by fMRI signal decreases. *NeuroImage* 17, 490–496.

Haslinger, B., Noe, J., Altenmuller, E., Riedel, V., Zimmer, C., Mantel, T., Dresel, C., 2016. Changes in Resting-State Connectivity in Musicians with Embouchure Dystonia. (*Mov. Disord.*)

Himberg, J., Hyvarinen, A., Esposito, F., 2004. Validating the independent components of neuroimaging time series via clustering and visualization. *NeuroImage* 22, 1214–1222.

Hoshi, E., Tanji, J., 2007. Distinctions between dorsal and ventral premotor areas: anatomical connectivity and functional properties. *Curr. Opin. Neurobiol.* 17, 234–242.

Hubsch, C., Roze, E., Popa, T., Russo, M., Balachandran, A., Pradeep, S., Mueller, F., Brochard, V., Quartarone, A., Degos, B., Vidailhet, M., Kishore, A., Meunier, S., 2013. Defective cerebellar control of cortical plasticity in writer's cramp. *Brain* 136, 2050–2062.

Ibanez, V., Sadato, N., Karp, B., Deiber, M.P., Hallett, M., 1999. Deficient activation of the motor cortical network in patients with writer's cramp. *Neurology* 53, 96–105.

Kelly Jr, R.E., Alexopoulos, G.S., Wang, Z., Gunning, F.M., Murphy, C.F., Morimoto, S.S., Kanellopoulos, D., Jia, Z., Lim, K.O., Hoptman, M.J., 2010. Visual inspection of independent components: defining a procedure for artifact removal from fMRI data. *J. Neurosci. Methods* 189, 233–245.

Koch, W., Teipel, S., Mueller, S., Benninghoff, J., Wagner, M., Bokde, A.L., Hampel, H., Coates, U., Reiser, M., Meindl, T., 2012. Diagnostic power of default mode network resting state fMRI in the detection of Alzheimer's disease. *Neurobiol. Aging* 33, 466–478.

Laird, A.R., Fox, P.M., Eickhoff, S.B., Turner, J.A., Ray, K.L., McKay, D.R., Glahn, D.C., Beckmann, C.F., Smith, S.M., Fox, P.T., 2011. Behavioral interpretations of intrinsic connectivity networks. *J. Cogn. Neurosci.* 23, 4022–4037.

Langbour, N., Michel, V., Dilharreguy, B., Guehl, D., Allard, M., Burbaud, P., 2017. The cortical processing of sensorimotor sequences is disrupted in writer's cramp. *Cereb. Cortex* 27, 2544–2559.

LeDoux, M.S., Brady, K.A., 2003. Secondary cervical dystonia associated with structural lesions of the central nervous system. *Mov. Disord.* 18, 60–69.

Lerner, A., Shill, H., Hanakawa, T., Bushara, K., Goldfine, A., Hallett, M., 2004. Regional cerebral blood flow correlates of the severity of writer's cramp symptoms.

- NeuroImage 21, 904–913.
- Magri, C., Schridde, U., Murayama, Y., Panzeri, S., Logothetis, N.K., 2012. The amplitude and timing of the BOLD signal reflects the relationship between local field potential power at different frequencies. *J. Neurosci.* 32, 1395–1407.
- Meunier, S., Garnero, L., Ducorps, A., Mazieres, L., Lehericy, S., du Montcel, S.T., Renault, B., Vidailhet, M., 2001. Human brain mapping in dystonia reveals both endophenotypic traits and adaptive reorganization. *Ann. Neurol.* 50, 521–527.
- Mink, J.W., 1996. The basal ganglia: focused selection and inhibition of competing motor programs. *Prog. Neurobiol.* 50, 381–425.
- Mohammadi, B., Kollewe, K., Samii, A., Beckmann, C.F., Dengler, R., Munte, T.F., 2012. Changes in resting-state brain networks in writer's cramp. *Hum. Brain Mapp.* 33, 840–848.
- Moore, R.D., Gallea, C., Horowitz, S.G., Hallett, M., 2012. Individuated finger control in focal hand dystonia: an fMRI study. *NeuroImage* 61, 823–831.
- Nagai, Y., Critchley, H.D., Featherstone, E., Fenwick, P.B., Trimble, M.R., Dolan, R.J., 2004. Brain activity relating to the contingent negative variation: an fMRI investigation. *NeuroImage* 21, 1232–1241.
- Naumann, M., Magyar-Lehmann, S., Reiners, K., Erbguth, F., Leenders, K.L., 2000. Sensory tricks in cervical dystonia: perceptual dysbalance of parietal cortex modulates frontal motor programming. *Ann. Neurol.* 47, 322–328.
- Nelson, A.J., Blake, D.T., Chen, R., 2009. Digit-specific aberrations in the primary somatosensory cortex in writer's cramp. *Ann. Neurol.* 66, 146–154.
- Nelson, A.J., Hoque, T., Gunraj, C., Ni, Z., Chen, R., 2010. Impaired interhemispheric inhibition in writer's cramp. *Neurology* 75, 441–447.
- Neumann, W.J., Jha, A., Bock, A., Huebel, J., Horn, A., Schneider, G.H., Sander, T.H., Litvak, V., Kuhn, A.A., 2015. Cortico-pallidal oscillatory connectivity in patients with dystonia. *Brain* 138, 1894–1906.
- Neychev, V.K., Fan, X., Mitev, V.I., Hess, E.J., Jinnah, H.A., 2008. The basal ganglia and cerebellum interact in the expression of dystonic movement. *Brain* 131, 2499–2509.
- Neychev, V.K., Gross, R.E., Lehericy, S., Hess, E.J., Jinnah, H.A., 2011. The functional neuroanatomy of dystonia. *Neurobiol. Dis.* 42, 185–201.
- Niehaus, L., von Alt-Stutterheim, K., Roricht, S., Meyer, B.U., 2001. Abnormal post-excitatory and interhemispheric motor cortex inhibition in writer's cramp. *J. Neurol.* 248, 51–56.
- Nowak, D.A., Rosenkranz, K., Topka, H., Rothwell, J., 2005. Disturbances of grip force behaviour in focal hand dystonia: evidence for a generalised impairment of sensory-motor integration? *J. Neurol. Neurosurg. Psychiatry* 76, 953–959.
- Odergren, T., Stone-Elander, S., Ingvar, M., 1998. Cerebral and cerebellar activation in correlation to the action-induced dystonia in writer's cramp. *Mov. Disord.* 13, 497–508.
- Oga, T., Honda, M., Toma, K., Murase, N., Okada, T., Hanakawa, T., Sawamoto, N., Nagamine, T., Konishi, J., Fukuyama, H., Kaji, R., Shibasaki, H., 2002. Abnormal cortical mechanisms of voluntary muscle relaxation in patients with writer's cramp: an fMRI study. *Brain* 125, 895–903.
- Peller, M., Zeuner, K.E., Munchau, A., Quartarone, A., Weiss, M., Knutzen, A., Hallett, M., Deuschl, G., Siebner, H.R., 2006. The basal ganglia are hyperactive during the discrimination of tactile stimuli in writer's cramp. *Brain* 129, 2697–2708.
- Power, J.D., Mitra, A., Laumann, T.O., Snyder, A.Z., Schlaggar, B.L., Petersen, S.E., 2014. Methods to detect, characterize, and remove motion artifact in resting state fMRI. *NeuroImage* 84, 320–341.
- Preibisch, C., Berg, D., Hofmann, E., Solymosi, L., Naumann, M., 2001. Cerebral activation patterns in patients with writer's cramp: a functional magnetic resonance imaging study. *J. Neurol.* 248, 10–17.
- Quartarone, A., Hallett, M., 2013. Emerging concepts in the physiological basis of dystonia. *Mov. Disord.* 28, 958–967.
- Rajapakse, J.C., Giedd, J.N., Rapoport, J.L., 1997. Statistical approach to segmentation of single-channel cerebral MR images. *IEEE Trans. Med. Imaging* 16, 176–186.
- Restuccia, D., Valeriani, M., Barba, C., Le Pera, D., Capecchi, M., Filippini, V., Molinari, M., 2001. Functional changes of the primary somatosensory cortex in patients with unilateral cerebellar lesions. *Brain* 124, 757–768.
- Rijntjes, M., Dettmers, C., Buchel, C., Kiebel, S., Frackowiak, R.S., Weiller, C., 1999. A blueprint for movement: functional and anatomical representations in the human motor system. *J. Neurosci.* 19, 8043–8048.
- Rizzolatti, G., Fogassi, L., Gallese, V., 2002. Motor and cognitive functions of the ventral premotor cortex. *Curr. Opin. Neurobiol.* 12, 149–154.
- Scheperjans, F., Eickhoff, S.B., Homke, L., Mohlberg, H., Hermann, K., Amunts, K., Zilles, K., 2008. Probabilistic maps, morphometry, and variability of cytoarchitectonic areas in the human superior parietal cortex. *Cereb. Cortex* 18, 2141–2157.
- Schluter, N.D., Rushworth, M.F., Passingham, R.E., Mills, K.R., 1998. Temporary interference in human lateral premotor cortex suggests dominance for the selection of movements. A study using transcranial magnetic stimulation. *Brain* 121 (Pt 5), 785–799.
- Shakkottai, V.G., Batla, A., Bhatia, K., Dauer, W.T., Dresel, C., Niethammer, M., Eidelberg, D., Raikie, R.S., Smith, Y., Jinnah, H.A., Hess, E.J., Meunier, S., Hallett, M., Fremont, R., Khodakhah, K., LeDoux, M.S., Popa, T., Gallea, C., Lehericy, S., Bostan, A.C., Strick, P.L., 2017. Current opinions and areas of consensus on the role of the cerebellum in dystonia. *Cerebellum* 16, 577–594.
- Sheehy, M.P., Marsden, C.D., 1982. Writers' cramp—a focal dystonia. *Brain* 105 (Pt 3), 461–480.
- Smith, S.M., Fox, P.T., Miller, K.L., Glahn, D.C., Fox, P.M., Mackay, C.E., Filippini, N., Watkins, K.E., Toro, R., Laird, A.R., Beckmann, C.F., 2009. Correspondence of the brain's functional architecture during activation and rest. *Proc. Natl. Acad. Sci. U. S. A.* 106, 13040–13045.
- Stamelou, M., Edwards, M.J., Hallett, M., Bhatia, K.P., 2012. The non-motor syndrome of primary dystonia: clinical and pathophysiological implications. *Brain* 135, 1668–1681.
- Tamburin, S., Fiaschi, A., Marani, S., Andreoli, A., Manganotti, P., Zanette, G., 2004. Enhanced intracortical inhibition in cerebellar patients. *J. Neurol. Sci.* 217, 205–210.
- Wu, X., Li, R., Fleisher, A.S., Reiman, E.M., Guan, X., Zhang, Y., Chen, K., Yao, L., 2011. Altered default mode network connectivity in Alzheimer's disease—a resting functional MRI and Bayesian network study. *Hum. Brain Mapp.* 32, 1868–1881.